Structural, Spectroscopic, and Chemical Properties of the First Low-Spin Iron(III) Semiquinonate Complexes in the Solid State and in Solution

Welf O. Koch, Volker Schünemann, Michael Gerdan, Alfred X. Trautwein, and Hans-Jörg Krüger*

Dedicated to Professor Bernt Krebs on the occasion of his 60th birthday

Abstract: The reaction of iron(II) perchlorate with the tetraazamacrocyclic ligand *N*,*N*′-dimethyl-2,11-diaza[3.3](2,6)pyridinophane (L-N_4Me_2) and 3,5-di-*tert*-butyl-1,2-benzoquinone in 96% ethanol yields the blue compound $[Fe(L\text{-}N_4Me_2)(dbsq)](ClO_4)_2 \cdot 2.5\,H_2O$ (**3a**, $dbsq^- = 3,5$-di-*tert*-butyl-1,2-benzosemiquinonate). On the basis of structural, Mössbauer spectroscopic, and magnetic evidence, this compound was identified as a low-spin iron(III) semiquinonate complex, the first of its kind, in which the unpaired electron of the coordinated semiquinonate radical is strongly antiferromagnetically coupled with the unpaired electron of the low-spin iron(III) ion. In acetonitrile solution, $[Fe(L\text{-}N_4Me_2)(dbsq)]^{2+}$ (**3**) is in equilibrium with uncoordinated dbq and with the low-spin iron(II) complex $[Fe(L\text{-}N_4Me_2)(MeCN)_2]^{2+}$ (**5**), as demonstrated by NMR, Mössbauer, and UV/Vis spectroscopic data, as well as by the electrochemical results. The equilibrium constant for the reaction $\mathbf{3} + 2\,MeCN \rightleftharpoons dbq + \mathbf{5}$ was determined to be $7.97 \times 10^{-6}\,M^{-1}$ at 25 °C, and the pseudo-first-order rate constant for the forward reaction $k = k_f[MeCN]^2$ to be $2.85\,s^{-1}$ by NMR spectroscopy and electrochemical methods, respectively. This equilibrium constant and the redox potentials, determined for the involved species, were used to calculate the formation constants for the complexation of $dbsq^-$ and 3,5-di-*tert*-butylcatecholate (dbc^{2-}) by $[Fe(L\text{-}N_4Me_2)(MeCN)_2]^{2+,\,3+}$ ions. Solutions of complex **3** in acetonitrile are found to be stable towards molecular oxygen. In addition, the reaction of the iron(III) semiquinonate complex **3** with superoxide quantitatively yields the corresponding iron(III) catecholate complex $[Fe(L\text{-}N_4Me_2)(dbc)]^+$ (**2**). Therefore, the reactivity of **3** with molecular oxygen and with superoxide demonstrates that the correct oxidation states of *both* the metal ion *and* the coordinated dioxolene unit are required for the occurrence of the well-established cleavage of the *intradiol* C–C bond of 3,5-di-*tert*-butylcatecholate ligand coordinated to the iron(III) ion in **2** by molecular oxygen and that the cleavage reaction does not occur through an initial electron-transfer step, resulting in the formation of an iron(III) semiquinonate as intermediate, but instead by the direct attack of the oxygen molecule on the iron(III) catecholate moiety.

Keywords: iron · macrocyclic ligands · radical ions · redox chemistry · semiquinonate ligands

Introduction

Ligand radicals coordinated to metal ions are gaining in importance within the discussion of the reactivity and structural and electronic features of active sites in metalloproteins; recently it was recognized that the mononuclear copper site in the oxidized form of the enzyme galactose oxidase consists of a copper(II) center coordinated to a phenoxyl radical and not a copper(III) ion as had been previously presumed.[1] Since that discovery substantial effort has focussed on investigating the coordination of phenoxyl radicals to metal ions.[2] It has already been established that the formally pentavalent iron ion in the active sites of cytochrome *P*450 and horseradish peroxidase is actually an iron(IV) oxo species bound to a cationic porphyrin radical.[3] Furthermore, the unusual reactivity of molecular oxygen with the iron(III) catecholate complex of intradiol-cleaving catechol dioxygenases has been attributed to a partial transfer of electron density from the coordinated catecholate to the metal ion, whereby the active site is endowed with a partial iron(II) semiquinonate character, which is thought to be responsible for the reactivity.[4]

We have recently reported[5] on the synthesis and reactivity of the iron(III) catecholate (cat^{2-}) and 3,5-di-*tert*-butylcatecholate (dbc^{2-}) complexes **1** and **2**, which contain the

[*] Priv. Doz. Dr. H.-J. Krüger, W. O. Koch
Institut für Anorganische und Angewandte Chemie
der Universität Hamburg
Martin-Luther-King-Platz 6, D-20146 Hamburg (Germany)
Fax: (+ 49) 40-41232893
E-mail: krueger@xray.chemie.uni-hamburg.de
Dr. V. Schünemann, Michael Gerdan, Prof. Dr. A. X. Trautwein
Institut für Physik
der Medizinischen Universität zu Lübeck (Germany)

 © WILEY-VCH Verlag GmbH, D-69451 Weinheim, 1998 0947-6539/98/0407-1255 $ 17.50+.25/0

tetraazamacrocycle *N*,*N*′-dimethyl-2,11-diaza[3.3](2,6)pyridinophane (L-N_4Me_2) as a coligand. In the reaction with molecular oxygen, the aromatic ring of the coordinated

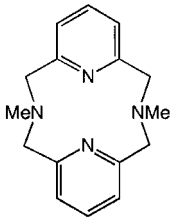

L–N_4Me_2

$[Fe(L–N_4Me_2)(cat)]^+$

1

$[Fe(L–N_4Me_2)(dbc)]^+$

2

$[Fe(L–N_4Me_2)(dbsq)]^{2+}$

3

catecholate moiety in these complexes was shown to be oxidatively cleaved at the intradiol C–C bond in quantitative yields. In addition to the stoichiometric reaction, complex **2** acts as an efficient catalyst in the conversion of $dbcH_2$ to 3,5-di-*tert*-butylmuconic anhydride. Thus, with complex **2**, we introduced a well-defined, stoichiometrically functioning, *and* highly catalytic biomimetic model system for the reactivity of intradiol-cleaving catechol dioxygenases.

By virtue of belonging to the class of dioxolenes, coordinated catecholates are prone to behave like non-innocent ligands,[6] a property which may, as previously mentioned, be pertinent to the reactivity of catechol dioxygenases. Since in most complexes the metal d orbital and the π-molecular orbital of the dioxolene are of comparable energies, valence tautomerism can occur. Thus, if the concept of formal oxidation states is used—although it may not always be appropriate—the electron distribution in a given metal–dioxolene complex could be described by any one of the three depicted redox isomers: a catecholate, a semiquinonate, or a quinone complex. Which of these redox states is actually the most

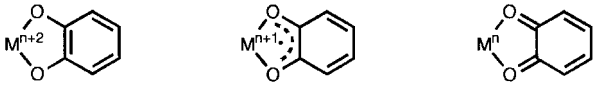

applicable description for a coordinated dioxolene unit, is determined by the covalency of the metal–oxygen bonds—which again depends on the relative energies, the symmetries, and the overlap of the involved metal d orbitals and the π-molecular orbitals on the dioxolene unit. Since redox reactions can involve the metal ion as well as the ligand, a rich redox chemistry is associated with this class of complexes.

Within the context of our studies on functional biomimetic complexes that model the reactivity of intradiol-cleaving catechol dioxygenases, we were also interested in the complex $[Fe(L\text{-}N_4Me_2)(dbsq)]^{2+}$ (**3**; $dbsq^- =$ 3,5-di-*tert*-butyl-1,2-benzosemiquinonate), which is the one-electron oxidation product of **2**. The finding that the reaction of complex **2** with molecular oxygen indeed affords high yields of intradiol-cleavage products, and the previously mentioned working hypothesis that the coordinated dioxolene unit in **2** needs some semiquinonate radical character in order to be reactive with molecular oxygen, prompted us to investigate the reaction chemistry of the radical ligand 3,5-di-*tert*-butylsemiquinonate coordinated to a (diazapyridinophane)iron(III) fragment. Here we report on the structural and electronic properties as well as the reactivity of **3**, which, to our knowledge, is the first low-spin iron(III) semiquinonate complex ever reported.

Results and Discussion

Synthesis and structure: Analogous to the preparation of previously reported iron(III) semiquinonate complexes,[7] $[Fe(L\text{-}N_4Me_2)(dbsq)](ClO_4)_2 \cdot 2.5\,H_2O$ (**3a**) was synthesized by addition of 3,5-di-*tert*-butyl-1,2-benzoquinone (dbq) to an ethanolic solution containing equivalent amounts of ferrous perchlorate and the tetraazamacrocyclic ligand L-N_4Me_2. The presence of 2.5 molecules of water per molecule of complex is supported by elemental analysis as well as by an X-ray structure determination of single crystals obtained by recrystallization of the dark blue compound from hot 96% ethanol. Unfortunately the quality of the single crystals of **3a** was poor due to some severe disorder in the crystal lattice; therefore, for the sole purpose of obtaining suitable crystals, the complex was additionally prepared as the hexafluorophosphate salt $[Fe(L\text{-}N_4Me_2)(dbsq)](PF_6)_2$ (**3b**).

A perspective view of **3** with the atom numbering scheme is shown in Figure 1. A comparison of some selected distances

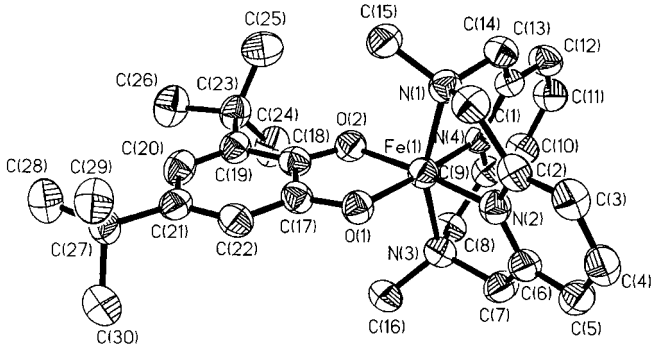

Figure 1. Perspective view of the structure of $[Fe(L\text{-}N_4Me_2)(dbsq)]^{2+}$ in **3a** showing thermal ellipsoids at 50% probability and the atom-numbering scheme.

and angles of the complex with those of the ferric catecholate complexes **1** and **2**[5, 8] is given in Table 1.

As in the iron(III) catecholate complexes, a distorted *cis* octahedral coordination geometry is also found around the iron ion in **3**; the dioxolene moiety is coordinated in the equatorial plane to the metal ion in a bidentate fashion. The average $Fe–N_{amine}$ and $Fe–N_{py}$ bond lengths of 2.026 ± 0.004 and 1.894 ± 0.002 Å, respectively, are considerably shorter than those found in the iron(III) catecholate complexes or in all previously investigated octahedral high-spin iron(III) complexes with L-N_4Me_2 in their ligand spheres ($Fe–N_{amine}$: 2.223–2.243 Å and $Fe–N_{py}$: 2.106–2.152 Å).[5, 9] Compared to the commonly observed Fe–N bond lengths in octahedral high-spin iron(III) complexes, the substantial difference in the bond lengths (about 0.2 Å) could indicate that upon addition of *o*-benzoquinone to the iron(II) complex either the metal ion is oxidized by two electrons to an iron(IV) ion, or a low-spin

© WILEY-VCH Verlag GmbH, D-69451 Weinheim, 1998
0947-6539/98/0407-1256 $ 17.50+.50/0 *Chem. Eur. J.* **1998**, *4*, No. 7

Table 1. Selected bond lengths [Å] and angles [°] in **1**–**3**.

	1	**2**	**3**
Fe(1)–O(1)	1.903(3)	1.895(5)	1.883(3)
Fe(1)–O(2)	1.915(3)	1.911(5)	1.885(3)
Fe(1)–N(1)	2.222(3)	2.241(6)	2.022(4)
Fe(1)–N(2)	2.105(3)	2.121(6)	1.892(4)
Fe(1)–N(3)	2.223(3)	2.235(6)	2.030(4)
Fe(1)–N(4)	2.106(3)	2.115(6)	1.895(4)
O(1)–C(17)	1.353(5)	1.344(8)	1.284(5)
O(2)–C(18)	1.329(5)	1.368(8)	1.296(5)
C(17)–C(18)	1.415(7)	1.411(10)	1.450(7)
C(17)–C(22)	1.385(7)	1.380(10)	1.403(7)
C(18)–C(19)	1.394(6)	1.409(10)	1.425(7)
C(19)–C(20)	1.369(8)	1.396(10)	1.370(7)
C(20)–C(21)	1.369(9)	1.399(10)	1.438(7)
C(21)–C(22)	1.427(8)	1.393(10)	1.360(7)
O(1)-Fe(1)-O(2)	85.6(1)	85.1(2)	83.7(1)
O(1)-Fe(1)-N(1)	97.7(1)	105.1(2)	97.4(2)
O(1)-Fe(1)-N(2)	100.4(1)	95.4(2)	89.7(2)
O(1)-Fe(1)-N(3)	107.3(1)	98.3(2)	99.0(2)
O(1)-Fe(1)-N(4)	174.7(1)	174.1(2)	176.0(2)
O(2)-Fe(1)-N(1)	103.7(1)	104.4(2)	100.1(2)
O(2)-Fe(1)-N(2)	173.7(1)	178.2(2)	173.3(2)
O(2)-Fe(1)-N(3)	99.0(1)	100.8(2)	96.6(2)
O(2)-Fe(1)-N(4)	93.0(1)	99.5(2)	92.3(2)
N(1)-Fe(1)-N(2)	77.4(1)	77.2(2)	81.3(2)
N(1)-Fe(1)-N(3)	147.3(1)	146.8(2)	157.7(2)
N(1)-Fe(1)-N(4)	77.6(1)	77.6(2)	83.2(2)
N(2)-Fe(1)-N(3)	77.6(1)	77.4(2)	83.7(2)
N(2)-Fe(1)-N(4)	81.1(1)	79.9(2)	94.4(2)
N(3)-Fe(1)-N(4)	77.9(1)	77.3(2)	81.5(2)

iron(III) ion is present in complex **3**. The first possibility, which would have been unprecedented in the literature, can be excluded on the basis of the structural parameters of the coordinated dioxolene ligand and on the basis of the spectroscopic evidence (vide infra). In fact the Fe–N bonds are quite similar to those in $[Fe(L\text{-}N_4Me_2)(bipy)]^{3+}$, which also contains a low-spin iron(III) ion ($Fe-N_{amine}$: 2.044 Å and $Fe-N_{py}$: 1.902 Å).[9]

A comparison of the C–O and C–C bond lengths (Table 1) with those of the iron(III) catecholate complexes clearly attributes semiquinonato character to the dioxolene ligand. Thus, upon oxidation of **2**, the C–O bond lengths significantly decrease to 1.284 and 1.296 Å, thereby falling into the range commonly observed for coordinated semiquinonato radicals.[6, 7, 10] While the more or less equal lengths of the C–C bonds within the catecholate ligands of **1** and **2** are consistent with an aromatic ring system with delocalized π bonds, an inspection of the C–C bonds in **3** reveals the more localized π-bonding pattern of an *ortho*-semiquinone. Therefore, short bond lengths of 1.36–1.37 Å are observed for the C(19)–C(20) and C(21)–C(22) bonds. On the other hand, the C(17)–C(18) and C(20)–C(21) bonds are considerably lengthened (1.44–1.45 Å). Considering that the dioxolene moiety can be unambiguously identified as a semiquinonate, the short Fe–N bonds must therefore result from the low-spin state of the iron(III) ion. The effect of the low-spin state is also expressed in the extremely short Fe–O bonds (1.883 and 1.885 Å), whereas all reported high-spin iron(III) semiquinonate complexes display Fe–O bond lengths between 2.0 and 2.1 Å.[7, 10] A theoretically possible assignment of complex **3** as a low-spin iron(II) quinone complex was excluded from further consideration on the basis of the C–O bond lengths and, more importantly, on the basis of the Mössbauer data (vide infra).

Compared to high-spin iron(III) complexes with the ligand $L\text{-}N_4Me_2$, the unusually short Fe–N bonds cause the metal ion to be drawn into the cavity of the macrocycle to a larger extent, thereby increasing the $N_{amine}\text{-}Fe\text{-}N_{amine}$ and the $N_{py}\text{-}Fe\text{-}N_{py}$ angles from 147° to 158° and from 80° to 94°. As in all complexes with $L\text{-}N_4Me_2$ ligands,[11] the interplanar angle included by the least-squares planes of the pyridine rings is smaller than the $N_{py}\text{-}M\text{-}N_{py}$ angle; however, in **3** this angle is 82°, which is one of the largest observed in complexes containing $L\text{-}N_4Me_2$. Thus, the metal ion is considerably less displaced from the least-squares planes of the pyridine rings. These findings serve as evidence that the tetraazamacrocyclic ligand still provides sufficient flexibility to accommodate the individual electronic requirements of the respective coordinated iron ion, in spite of the steric rigidity induced by the pyridine rings.

Properties of the iron(III) semiquinonate complex in the solid state: The Mössbauer spectrum (Figure 2) of solid **3a**, recorded at 4.2 K, consists of a doublet with an isomer shift

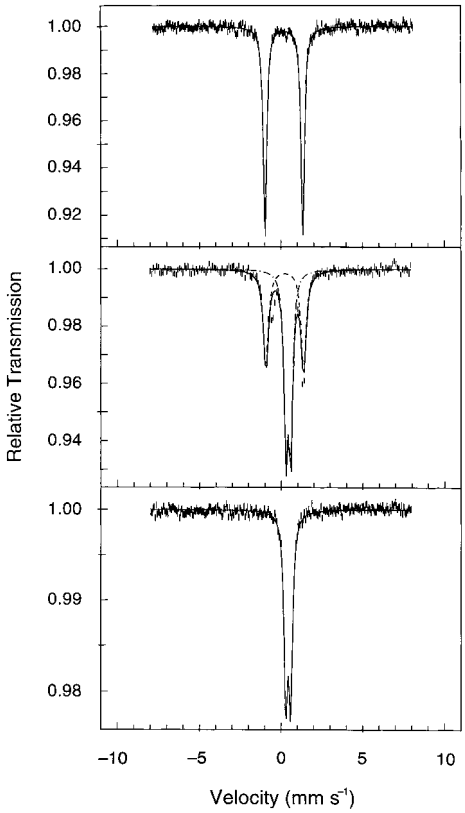

Figure 2. Mössbauer spectra (recorded at 4.2 K) of $[Fe(L\text{-}N_4Me_2)(dbsq)]^{2+}$ as a solid (top), $[^{57}Fe(L\text{-}N_4Me_2)(dbsq)]^{2+}$ electrochemically generated in acetonitrile solution (2 mM, middle), and $[Fe(L\text{-}N_4Me_2)(MeCN)_2]^{2+}$ (bottom), generated in situ, in acetonitrile.

$\delta = 0.18\ mm\,s^{-1}$ and a quadrupole splitting $\Delta E_Q = 2.32\ mm\,s^{-1}$. Compared to the usually observed range of $\delta = 0.4$–$0.6\ mm\,s^{-1}$ for other six-coordinate high-spin iron(III) complexes containing this tetraazamacrocyclic ligand, the present value for δ is significantly reduced. Also taking into account

the relatively high value for ΔE_Q, the Mössbauer data confirm the low-spin Fe^{III} state which was established earlier by the X-ray structure analysis. An additional measurement of **3a** at 4.2 K with an applied field of 6.1 T $\perp \gamma$ (not shown) clearly attributes a diamagnetic ground state to the complex. Furthermore, it reveals a negative sign for the electric field gradient. The diamagnetism of the complex indicates a strong *intra*molecular antiferromagnetic coupling between the $S_1 = 1/2$ spin of the low-spin iron(III) ion and the $S_2 = 1/2$ spin located on the coordinated semiquinone radical. By using a spin Hamiltonian $H = -2JS_1S_2$ for the interaction between the two electron spins S_1 and S_2, a magnetic exchange coupling constant of $|-J| > 250\ cm^{-1}$ can be estimated from the measurements of the magnetic susceptibility of solid **3a** in the temperature range $2\,K < T < 293\,K$ by using a SQUID magnetometer. It is noteworthy that complex **3** is, to our knowledge, the first low-spin iron(III) semiquinonate complex ever isolated and structurally characterized; all other previously reported iron(III) semiquinonate complexes contain a high-spin iron(III) ion.[7, 10]

Properties of dissolved iron(III) semiquinonate complexes: The spectroscopic and the electrochemical properties of **3** in acetonitrile were investigated. These properties were compared with those of an analogous complex $[Fe(L\text{-}N_4Me_2)(sq)]^{2+}$ (**4**), which contains the unsubstituted *o*-benzosemiquinonate (sq^-) ligand. Complex **4** was generated electrochemically from **1** in acetonitrile, these solutions were generally handled only at low temperatures because of the instability **4**.

NMR spectroscopic investigations: ^1H NMR spectra of 10 mM solutions of **3a** were recorded at different temperatures in deuterated acetonitrile. The NMR signals lie between 1 and 9 ppm and display small linewidths at low temperatures, which indicates that only diamagnetic compounds are present. As the temperature was increased, some of the signals broadened and shifted. This could result from the appearance of a paramagnetic species at higher temperatures or it could be caused by some dynamic process(es).

From the changing intensities of the signals with varying temperature, it is concluded that the overall NMR spectrum originates from three different compounds: these have been unambiguously identified as **3**, $[Fe(L\text{-}N_4Me_2)(MeCN)_2]^{2+}$ (**5**), and unbound dbq. Analogously, the NMR signals in the spectrum of an electrochemically generated sample of **4** are attributed to uncoordinated 1,2-benzoquinone (q) and to complexes **4** and **5**. The spectrum of **3a** in acetonitrile (recorded at $-30\,^\circ C$) is displayed in Figure 3, and the assignments of the individual NMR signals in the spectra of **3** and **4** in acetonitrile are listed in Table 2.

The subspectrum corresponding to **3** is consistent with the $S = 0$ spin state, which has been previously discussed for the solid ferric semiquinonate complex. As in the spectra of other diamagnetic complexes containing the ligand $L\text{-}N_4Me_2$,[11] the low-field shift of the ^1H NMR signals of the pyridine protons (compared to those of unbound ligand) and the appearance of the characteristic AB coupling pattern for the diastereotopic methylene protons show that, as the complex **3** dissolves, the tetraazamacrocyclic ligand continues to be coordinated through all four nitrogen donor atoms to the iron ion. A similar conclusion is reached for the coordination mode of the macrocyclic ligand in **4**. The introduction of two *tert*-butyl substituents at the 3- and 5-positions of the semiquinonate ring reduces the symmetry of the complex from C_{2v} in **4** to C_s in **3**. Thus, in contrast to **4**, where only one AB signal is observed in the ^1H NMR spectrum, the presence of two slightly different AB signals in the spectrum of **3** reflects the lower symmetry of the coordinated $dbsq^-$ moiety.

Based on the low-field shifts of the NMR signals of the pyridine protons, the subspectrum attributed to complex **5**

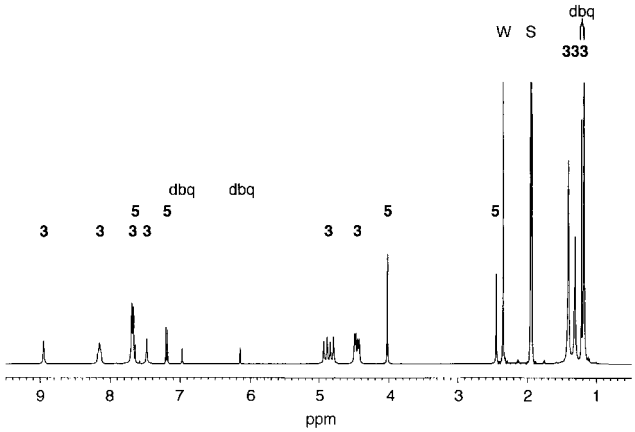

Figure 3. ^1H NMR spectrum of **3a** in deuterated acetonitrile (recorded at $-30\,^\circ C$ with $[\mathbf{3a}]_o = 10$ mM). The individual NMR signals corresponding to **3**, **5**, dbq, deuterated acetonitrile (S), and water (W) are marked.

Table 2. ^1H NMR data (360 MHz) of dbq, **3**–**5**, and 1,2-benzoquinone (q) in deuterated acetonitrile.

Compound	Temperature [°C]	Chemical shift [ppm]
dbq	25	1.22 (s, 9H, $C(CH_3)_3$), 1.25 (s, 9H, $C(CH_3)_3$), 6.16 (d, 1H, ArH, 2.3 Hz), 7.01 (d, 1H, ArH, 2.3 Hz).
3	−30	1.25 (s, 9H, $C(CH_3)_3$), 1.32 (s, 6H, NCH_3), 1.41 (s, 9H, $C(CH_3)_3$), 4.45 (d, 2H, -CH_2-, A-part of the first AB system, 17.0 Hz), 4.47 (d, 2H, -CH_2-, A-part of the second AB system, 17.1 Hz), 4.81 (d, 2H, -CH_2-, B-part of the second AB system, 17.1 Hz), 4.90 (d, 2H, -CH_2-, B-part of the first AB system, 17.0 Hz), 7.48 (s, 1H, ArH), 7.69 (two d, 4H, 3,5-py-H, 7.9 Hz), 8.15 (t, 1H, 4-pyH, 7.9 Hz), 8.16 (t, 1H, 4-pyH, 7.9 Hz), 8.95 (s, 1H, ArH).
4	−30	1.32 (s, 6H, NCH_3), 4.45 (d, 4H, -CH_2-, A-part of a AB system, 16.9 Hz), 5.01 (d, 4H, -CH_2-, B-part of a AB system, 16.9 Hz), 7.71 (d, 4H, 3,5-py-H, 7.6 Hz), 7.82 (m, 2H, ArH, AA′BB′ system, $J_{AA'} = 1.6$ Hz, $J_{AB} = 7.7$ Hz, $J_{AB'} = 2.9$ Hz), 8.16 (t, 2H, 4-pyH, 7.6 Hz), 9.23 (m, 2H, ArH, AA′BB′ system, $J_{BB'} = 1.6$ Hz, $J_{AB} = 7.7$ Hz, $J_{A'B} = 2.9$ Hz).
5	−30	2.45 (s, 6H, NCH_3), 4.02 (s, 8H, -CH_2-), 7.19 (d, 4H, 3,5-py-H, 7.7 Hz), 7.67 (t, 2H, 4-pyH, 7.7 Hz)
	25	2.63 (s, 6H, NCH_3), 4.03 (d, 4H, -CH_2-, A-part of a AB system, 16.5 Hz), 4.18 (d, 4H, -CH_2-, B-part of a AB system, 16.5 Hz), 7.30 (d, 4H, 3,5-py-H, 7.8 Hz), 7.70 (t, 2H, 4-pyH, 7.8 Hz).
q	−30	6.35 (m, 2H, ArH, AA′BB′ system, $J_{AA'} = 1.8$ Hz, $J_{AB} = 8.8$ Hz, $J_{AB'} = 3.1$ Hz), 7.12 (m, 2H, ArH, AA′BB′ system, $J_{BB'} = 1.8$ Hz, $J_{AB} = 8.8$ Hz, $J_{A'B} = 3.1$ Hz).

© WILEY-VCH Verlag GmbH, D-69451 Weinheim, 1998
0947-6539/98/0407-1258 $ 17.50+.50/0 *Chem. Eur. J.* **1998**, *4*, No. 7

(Table 2) reveals that the iron ion is coordinated to the tetraazamacrocyclic ligand L-N_4Me_2. At $-30\,^{\circ}C$, only a singlet at 4.03 ppm is observed for the diastereotopic methylene protons. However, when the temperature is raised, this accidental isochronicity of both protons is lifted and the expected AB signal appears. This provides unambiguous proof that the L-N_4Me_2 in this complex is also bound to the metal ion by all four nitrogen donor atoms. The relatively narrow linewidths at $-30\,^{\circ}C$ and the occurrence of the NMR signals between 1 and 9 ppm indicate that this iron complex is diamagnetic. At higher temperatures, however, the signals shift considerably and the linewidths increase to some extent. The NMR spectra of an equimolar mixture of ferrous perchlorate and L-N_4Me_2 in acetonitrile over the entire investigated temperature range showed identical chemical shifts and linewidths very similar to those observed in the subspectra corresponding to complex **5**. In contrast to acetonitrile solutions, the NMR spectrum of an equimolar mixture of ferrous perchlorate and the macrocyclic ligand in methanol indicates the formation of a paramagnetic complex. From this evidence, and taking into account that L-N_4Me_2 has a decisive tendency to form octahedral complexes, the composition of complex **5** is deduced to be $[Fe(L\text{-}N_4Me_2)(MeCN)_2]^{2+}$, in which, in addition to the macrocycle, two acetonitrile molecules are coordinated to a low-spin iron(II) ion. While, at $-30\,^{\circ}C$ in acetonitrile, complex **5** is essentially diamagnetic, the noticeable shifting of the NMR signals serves as evidence that, although the $S=0$ spin state still predominates, a small paramagnetic contribution, presumably due to the onset of a spin-crossover, is present at higher temperatures.

The third component in the mixture resulting from the dissolution of solid **3a** in acetonitrile is unequivocally identified as dbq by comparison of the NMR spectrum with that of an authentic sample in acetonitrile. Accordingly, in an electrochemically prepared solution of **4**, unbound *o*-benzoquinone (q) is found in addition to complexes **4** and **5**.

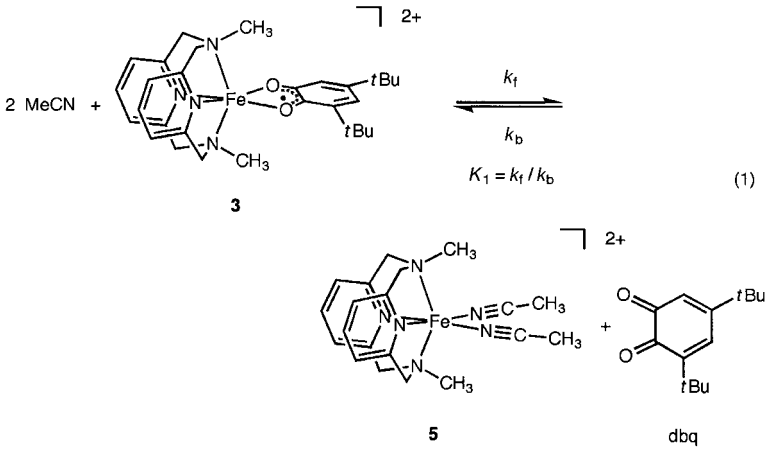

At all temperatures, compounds dbq and **5** are present in stoichiometrically equal amounts. From this it is inferred that **3** exists in an equilibrium with dbq and **5** [Eq. (1)]. From the intensities of the NMR signals, the equilibrium constant K_1 is determined to be $1.38\times10^{-6}\,M^{-1}$ and $7.19\times10^{-6}\,M^{-1}$ at $-30\,^{\circ}C$ and at $20\,^{\circ}C$, respectively. The temperature dependence of K_1 suggests that this reaction is endothermic and, from the stoichiometry of the reaction, a decrease in entropy is expected. Assuming that ΔH and ΔS are constant within the investigated temperature range (243 to 313 K in 10 K intervals), a plot of $\ln K_1$ against $1/T$ yields $\Delta H_1 = +20.0\,kJ\,mol^{-1}$ and $\Delta S_1 = -30.5\,J\,K^{-1}\,mol^{-1}$ for Equation (1). At $25\,^{\circ}C$, an equilibrium contant of $K_1 = 7.97\times10^{-6}\,M^{-1}$ was calculated.

As previously stated, the NMR signals attributed to **5** are shifted considerably when the temperature is changed. In contrast, the positions of the NMR signals of complex **3** are only slightly dependent on the temperature. The linewidths of the NMR signals of pure **5** and of **5** in the equilibrium mixture are very similar; therefore the noticeable line broadening of the NMR signals of **3** at higher temperatures ($>50\,^{\circ}C$) is judged to be due almost exclusively to the increasing paramagnetic contribution of **5** and not to a dynamic effect connected with the equilibrium reaction.

Since distinctive NMR signals are observed for each species at all temperatures, the intermolecular exchange processes of the protons due to the reaction in Equation (1) are in the slow exchange domain, which permits an estimate on the upper limit for the pseudo-first order rate constant $k = k_f/[MeCN]^2 < 20\,s^{-1}$. The occurrence of an equilibrium reaction is demonstrated further by two-dimensional exchange spectroscopy (EXSY) (not shown), with a mixing time t_M of 0.2 s at room temperature. The resulting spectrum not only gives further evidence for the correct assignment of the NMR signals, but also yields an approximate estimate for the rate constant $k = 0.5-5\,s^{-1}$.

For the electrochemically generated solution of **4**, an analogous equilibrium reaction is detected. Considering the well-known pervasive tendency of 1,2-benzoquinone to decompose at room temperature, this equilibrium reaction explains the difficulties experienced and the failure to synthesize and isolate **4** as a pure compound.

Mössbauer spectroscopic investigations: Mössbauer measurements were performed on solutions of **3a** in acetonitrile with initial concentrations between 0.4 and 20 mM as well as on a solution of **4** which was electrochemically generated from a 1.9 mM solution of **1** in acetonitrile. Figure 2 shows a comparison of the spectrum of a solution of **3a** (2 mM) with that of solid **3a**, and that of **5** generated in situ in acetonitrile. The experimental results are listed in Table 3. The spectra confirm that an equilibrium reaction occurs in solutions containing the iron(III) semiquinonate complexes. The rather similar Mössbauer parameters of **3** and **4** indicate similar structures for both complexes.

As expected, as the initial concentration of **3a** decreases, the equilibrium shifts to the side of the dissociation products. The equilibrium constant K_1 for the reaction in Equation (1), determined by Mössbauer spectroscopy, is slightly smaller than that obtained from the NMR data at $25\,^{\circ}C$. This is undoubtedly due to the fact that, during the short time required to rapidly freeze the samples,

Table 3. Mössbauer parameters for **3a**, **4**, and **5**.

Compound	δ [mm s^{-1}]	ΔE_Q [mm s^{-1}]	$\Gamma/2$ [mm s^{-1}]
solid **3a**			
	0.18	2.32	0.13
3a[b,c]	0.22	2.32	0.18 (43.3 %)
	0.44	0.30	0.14 (56.7 %)
4[b,d]	0.17	2.34	0.17 (34.6 %)
	0.42	0.30	0.13 (65.4 %)
5[b]	0.43	0.30	0.14

[a] $\Gamma/2$ = half-width of the lines. [b] As frozen solution in acetonitrile. [c] $[\mathbf{3a}]_o = 2.0$ mM. [d] $[\mathbf{4}]_o = 1.9$ mM.

the temperature of the solutions decreased before the frozen state was reached and, therefore, the established equilibria actually reflect temperature conditions lower than room temperature. The Mössbauer parameters for **5**, $\delta = 0.42$ mm s^{-1} and $\Delta E_Q = 0.30$ mm s^{-1}, are consistent with a low-spin iron(II) ion. In addition, the $S = 0$ spin state was confirmed experimentally by a measurement at 4 K with an applied field of 6.1 T $\perp \gamma$ (not shown).

Electronic absorption spectroscopy: Due to the equilibrium in Equation (1), the UV/Vis spectrum of a solution of **3a** in acetonitrile is composed of the electronic absorption spectra of three contributing species. Therefore, in order to obtain the electronic absorption spectrum corresponding exclusively to **3**, the molar extinction coefficients were determined of solutions of **5** (prepared in situ) and dbq in acetonitrile. The molar extinction coefficients obtained (listed in Table 4), the initial concentration of **3a**, and the equilibrium constant for

Table 4. Electronic absorption data for the complexes **3** and **5** as well as for dbq in acetonitrile.

Compound	Absorption maxima λ_{max} [nm] (ε_M)
3	351 (7620), 380 (sh, 5070), 600 (9360)
5	357 (4420), 381 (4510), 410 (sh, 2690), 475 (sh, 480), 580 (sh, 77.7)
dbq	401 (1730), 570 (45.8)

Equation (1) at 25 °C ($K_1 = 7.97 \times 10^{-6}$ M^{-1}) were used to calculate the electronic absorption spectrum of pure **3** (Table 4). The resulting molar extinction coefficients of pure **3**, obtained from measurements at two different initial concentrations of **3a** (10 and 1 mM), correspond closely to one another.

The spectrum shown in Figure 4 displays two intense absorption bands at 600 and 351 nm and a shoulder at 380 nm. The almost identical appearance of the spectrum of dissolved **3** to that of a solid sample supports the notion, already suggested by Mössbauer spectroscopic results, that the overall structure of the iron complex found in the solid state is preserved in solution. The position of the dominating transition at 600 nm does not show any marked solvent dependency [$\lambda = 611$ nm (solid state), 600 nm (MeCN), 595 nm (acetone), 604 nm (CH_2Cl_2), and 590 nm (EtOH)]. Because of the rather high intensity and the shift of this band to 550 nm in the absorption spectrum of **4** in acetonitrile, this band is tentatively assigned to a LMCT-transition. The rather

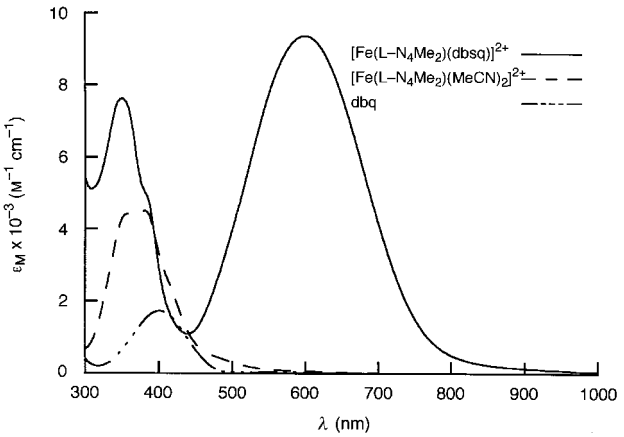

Figure 4. Electronic absorption spectra of **3**, **6**, and dbq in acetonitrile.

broad linewidth of approximately 5180 cm^{-1} indicates the occurrence of extensive vibrations in the excited state, which is consistent with the large reorganization energy associated with the strong CT character of the band. The resonance Raman spectrum of solid **3a** (excitation by a laser beam at $\lambda = 514$ nm), reveals strong features at $\nu = 576$, 604, 1373, and 1412 cm^{-1}, of which the first two are tentatively attributed to Fe–O stretching modes coupled to deformation vibrations of a five-membered chelate ring,[12] and the latter two to C–O and C–C stretching vibrations within the dioxolene moiety.[12a, 13] This result supports the involvement of a dioxolene ligand orbital in the CT transition at 600 nm.

UV/Vis spectra of iron(III)-3,5-di-*tert*-butylsemiquinonate complexes with a N_4O_2 coordination environment are rare and, to our knowledge, the only other case reported is that of the electrochemically generated complex [Fe(SS-CTH)(dbsq)]$^{2+}$ (**6**; SS-CTH = (*S*,*S*)-5,5,7,12,12,14-hexamethyl-1,4,8,11-tetraazacyclotetradecane).[14] Complex **6** does not show an absorption band at around 600 nm; instead, an absorption band was observed at 877 nm ($\varepsilon_M \approx 1700$ M^{-1} cm^{-1}). This transition has been attributed to an overlap of a CT transition and an internal ligand n-π*-transition (electronic absorption bands at rather similar energies have been observed for other metal complexes of the general stoichiometry [M(SS-CTH)(dbsq)]$^{n+}$ (with M = Ni^{2+}, Zn^{2+}, etc.)[15] as well as for electrochemically generated uncoordinated 3,5-di-*tert*-butylsemiquinonate).[16] For complex **3**, no such transition could be discerned at around 880 nm. Unfortunately, the spin state of **6** was not reported. However, we would like to speculate that these surprising dissimilarities in the absorption spectra of **3** and **6** might be the result of different spin states of the iron ions in these complexes and that **6** actually contains a high-spin iron(III) ion. In contrast, a quite intense absorption band at a rather similar position has been observed for [Ru(bipy)$_2$(dbq)]$^{2+}$ ($\lambda = 668$ nm, $\varepsilon = 14\,100$ M^{-1} cm^{-1})[17] and [Os(bipy)$_2$(dbsq)]$^{2+}$ ($\lambda = 558$ nm).[18] Since a low-spin osmium(III) ion is thought to be coordinated to a semiquinonate in the osmium complex, the absorption band was assigned to a LMCT transition. In contrast, based on the fact that the ruthenium complex is regarded as containing a low-spin ruthenium(II) ion coordinated to a benzoquinone, the band at 668 nm was assigned to a MLCT transition.

© WILEY-VCH Verlag GmbH, D-69451 Weinheim, 1998
0947-6539/98/0407-1260 $ 17.50+.50/0 *Chem. Eur. J.* **1998**, *4*, No. 7

However, the astounding similarities between the electronic absorption spectra of all three complexes with related N_4O_2 coordination spheres suggest that the transitions at around 600 nm may have the same origin. In default of a structure determination, the assignments of the oxidation states of the dioxolene ligand moiety and the ruthenium ion are, in our opinion, still uncertain.

Electrochemical investigation: At the outset, the electrochemical properties of uncoordinated dbq and of complex **5** in acetonitrile were determined by cyclic voltammetry. As shown in Equation (2), free 3,5-di-*tert*-butylbenzoquinone is reduced to the corresponding semiquinonate at a potential of $E_{1/2} = -0.51$ V vs. SCE, which is consistent with a previous investigation.[16] The cyclic voltammogram of complex **5**, generated in situ, demonstrates that an electrochemically reversible oxidation occurs at the rather high potential of $E_{1/2} = +1.06$ V vs. SCE (Equation (3)).

$$\mathrm{dbq} + e^- \underset{}{\overset{E_{1/2} = -0.51\ \mathrm{V}}{\rightleftharpoons}} \mathrm{dbsq}^- \qquad (2)$$

$$[\mathrm{Fe(L\text{–}N_4Me_2)(MeCN)_2}]^{3+} + e^- \overset{E_{1/2} = +1.06\ \mathrm{V}}{\rightleftharpoons} [\mathrm{Fe(L\text{–}N_4Me_2)(MeCN)_2}]^{2+} \qquad (3)$$

Cyclic voltammograms of **3a** dissolved in acetonitrile are presented in Figure 5. The existence of **5** as a consequence of the equilibrium in Equation (1) is demonstrated by the appearance of the oxidative response at $E_{1/2} = 1.06$ V (Figure 5a). Upon reduction, $[\mathrm{Fe(L\text{-}N_4Me_2)(dbsq)}]^{2+}$ is converted into $[\mathrm{Fe(L\text{-}N_4Me_2)(dbc)}]^{+}$ at a redox potential $E_{1/2} = 0.35$ V vs. SCE (Figure 5b). A scan to even lower potentials revealed a further peak potential at $E_{1/2} = -0.53$ V (not shown), which corresponds to the reduction of uncoordinated dbq to dbsq^-. With $[\mathbf{3a}]_o = 1.5$ mM, a current ratio $|i_{pc}/i_{pa}|$ of 0.63 was observed for the redox couple $[\mathrm{Fe(L\text{-}N_4Me_2)(dbsq)}]^{2+}/[\mathrm{Fe(L\text{-}N_4Me_2)(dbc)}]^{+}$. As predicted by the equilibrium in Equation (1), the relative concentration of **3** in the equilibrium mixture and with it the current ratio rises as uncoordinated dbq is added to the reaction mixture or as the initial concentration $[\mathbf{3a}]_o$ is increased. Thus, with $[\mathbf{3a}]_o = 1.5$ mM and $[\mathrm{dbq}]_o = 15$ mM (Figure 5b) and with $[\mathbf{3a}]_o = 10$ mM (Figure 5c), the current ratios $|i_{pc}/i_{pa}|$ are found to be 0.95 and 0.84, respectively. In agreement with the temperature dependency of the equilibrium in Equation (1), already established by NMR spectroscopy, the current ratio $|i_{pc}/i_{pa}|$ is also increased as the temperature is lowered (Figure 5d). Similar cyclic voltammograms are obtained for the redox reaction of the redox couple of $[\mathrm{Fe(L\text{-}N_4Me_2)(dbsq)}]^{2+}/[\mathrm{Fe(L\text{-}N_4Me_2)(dbc)}]^{+}$ starting from **2** (see Figure 6).

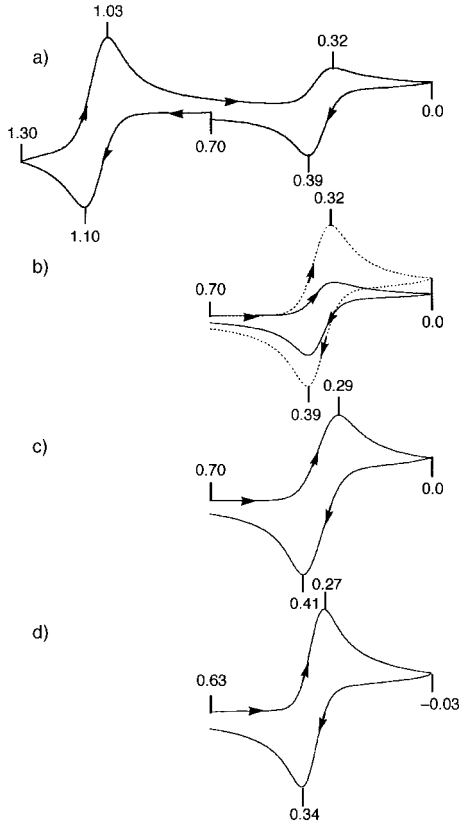

Figure 5. Cyclic voltammograms (50 mV s^{-1}) of **3a** at a Pt-foil electrode in acetonitrile a) with $[\mathbf{3a}]_o = 1.5$ mM (25 °C), b) with $[\mathbf{3a}]_o = 1.5$ mM before (solid line) and after (dotted line) the addition of dbq ($[\mathrm{dbq}]_o = 15$ mM (25 °C)), c) with $[\mathbf{3a}]_o = 10$ mM (25 °C), d) with $[\mathbf{3a}]_o = 1.5$ mM (−30 °C); peak potentials in V vs. SCE are indicated.

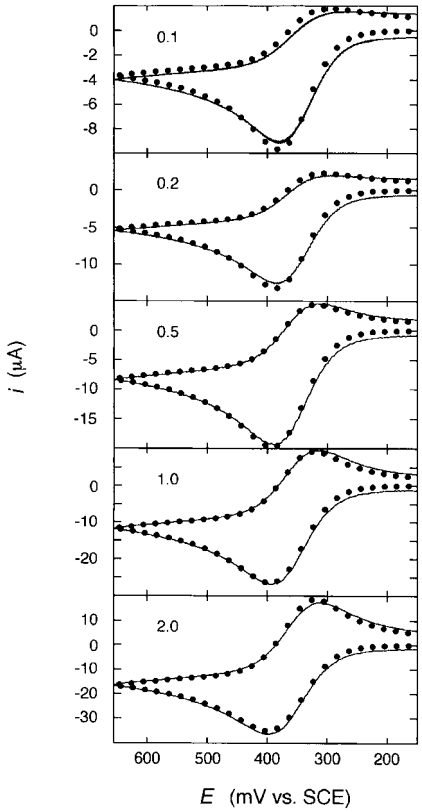

Figure 6. Experimental (solid line) and simulated (dotted line) cyclic voltammograms of $[\mathrm{Fe(L\text{-}N_4Me_2)(dbc)}](BPh_4)$ (1.53 mM) at a Pt-disc electrode (area = 33.9 mm^2) in acetonitrile at 25 °C (scan rate from top to bottom: 0.1 – 2.0 V s^{-1}).

Cyclic voltammograms of **2** and **3a** with different initial concentrations and at various scan rates were simulated, assuming identical diffusion coefficients for **2** and **3**. The diffusion coefficients of **2**, dbq, and **5** were determined by chronoamperometry.

In Figure 6, a selection of cyclic voltammograms and their corresponding simulations are displayed for the oxidation of **2**. They show that the redox kinetics are consistent with the E_rC_r mechanism shown by the reaction in Equation (4). Thus,

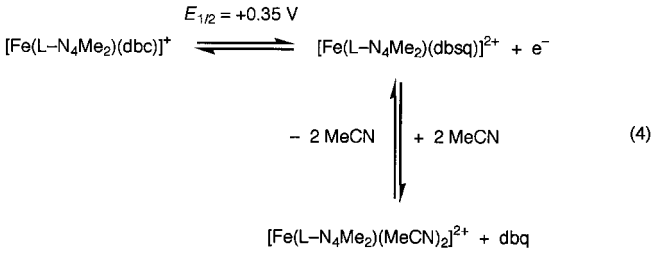

(4)

by increasing the scan rate v in the cyclic voltammetric experiment, the time scale of the experiment changes from a domain in which the chemical reaction is fast with respect to the electron transfer step (e.g. at $v = 0.1\ V s^{-1}$) to a range in which the chemical reaction is comparatively slow; therefore, the electron transfer reaction dominates the cyclic voltammetric response (e.g. at $v \geq 2\ V s^{-1}$). An optimal match between simulated and experimental data is obtained by using the pseudo-first-order rate constant for the chemical reaction $k = k_f/[MeCN]^2 = 2.85\ s^{-1}$, which agrees with those estimates acquired by NMR spectroscopy.

Electrolysis of complex **2** in acetonitrile at an applied potential of 0.47 V consumed 0.97 electrons per molecule; immediate re-reduction at 0.10 V, however, only accounted for 94 % of the originally transferred charge. The addition of a tenfold excess of dbq to the oxidized solution improved the yields in re-reduction to 99 %. This finding is interpreted to mean that the rate of electrolysis slowed considerably as the reduction progressed because the rate of the electron transfer depends on the actual number of molecules of $[Fe(L\text{-}N_4Me_2)(dbsq)]^{2+}$ available at the electrode surface, and because the back-reaction of the involved reversible chemical reaction is bimolecular. Addition of a tenfold excess of free dbq pushed the equilibrium of Equation (1) towards the side of the iron(III) semiquinonate complex, and, more importantly, thereby increased the rate of the back-reaction; therefore, the reduction is more complete within a reasonable electrolysis time.

Upon oxidation of **1** in acetonitrile at an applied potential of 0.62 V vs. SCE at $-40\,^{\circ}C$, a small residual current was observed after the passage of one electron per molecule. This indicates the presence of some redox-active compound, presumably generated by some decomposition reactions of the unsubstituted 1,2-benzoquinone, which is known for its instability. Immediate re-reduction of the solution oxidized by exactly one electron per molecule of **1** resulted in the recovery of 88 % of the originally transferred charge.

Determination of formation constants: The free energies (ΔG) and formation constants (K) for the complexation reactions of $dbsq^-$ and dbc^{2-} by the iron(II) and iron(III) complexes $[Fe(L\text{-}N_4Me_2)(MeCN)_2]^{n+}$ ($n = 2, 3$) in acetonitrile can be calculated and are listed in Table 5. Thus, the redox potentials of Equations (2) and (3) and the equilibrium constant of Equation (1) can be used to determine the free energy

Table 5. Thermodynamic data for various reactions in acetonitrile at 25 °C.

Reaction[a]	ΔG [kJ mol^{-1}]	K
1	29.1	7.97×10^{-6} M^{-1}
5	– 180.6	4.37×10^{31} M
6	– 112.1	4.36×10^{19} M
9	– 322.4	3.04×10^{56} M
10	– 160.3	1.21×10^{28} M

[a] Each of the given reactions refers to that in the corresponding Equation in the text.

$\Delta G = -180.6\ kJ\,mol^{-1}$ and the corresponding formation constant $K = 4.37 \times 10^{31}$ M for the reaction given in Equation (5) in acetonitrile at 25 °C. The major driving force for this reaction appears to be the large difference in redox potentials of the reactions in Equations (2) and (3).

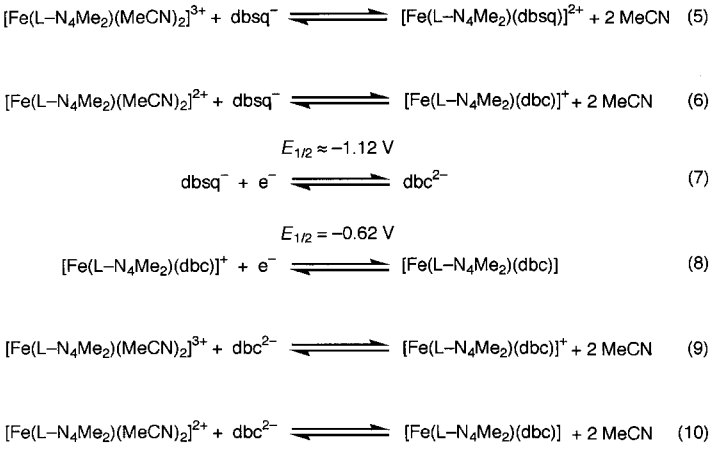

The free energy of the reaction in Equation (6) can be calculated with the potentials for the $[Fe(L\text{-}N_4Me_2)(dbsq)]^{2+}/[Fe(L\text{-}N_4Me_2)(dbc)]^{+}$ ($E_{1/2} = 0.35$ V vs. SCE) and $[Fe(L\text{-}N_4Me_2)(MeCN)_2]^{3+/2+}$ redox pairs. It is interesting to note that the formation constants for the complexation of $dbsq^-$ by the iron(II) and iron(III) complexes $[Fe(L\text{-}N_4Me_2)(MeCN)_2]^{n+}$ ($n = 2, 3$) in acetonitrile are several orders larger than those determined for several hydrated di- and trivalent metal ions in dimethylformamide.[16b]

The cyclic voltammogram of dbq in acetonitrile reveals that the reduction of $dbsq^-$ to dbc^{2-} [Eq. (7)] is electrochemically irreversible with a peak potential at -1.30 V.[16b] Therefore, an exact half-potential is not available. However, the reduction is electrochemically reversible in tetrahydrofuran.[19] Assuming that the separation between the potentials for the dbq/$dbsq^-$ and the $dbsq^-/dbc^{2-}$ redox couples stays approximately the same in acetonitrile and tetrahydrofuran, the redox potential for Equation (7) can be estimated to be -1.12 V vs SCE. With this value and the redox potential for the reduction of $[Fe(L\text{-}N_4Me_2)(dbc)]^{+}$ to $[Fe(L\text{-}N_4Me_2)(dbc)]$ [Eq. (8), $E_{1/2} = -0.62$ V vs. SCE],[8] the thermodynamics for the complexation of dbc^{2-} by $[Fe(L\text{-}N_4Me_2)(MeCN)_2]^{n+}$ ($n = 2, 3$) ions [Eqs. (9) and (10)] can be evaluated.

The equilibrium constants for the reactions in Equations (6) and (9) indicate that the catecholate ligand of complex **2** remains coordinated in solution. This finding suggests that neither uncoordinated $dbsq^-$ nor uncoordinated

© WILEY-VCH Verlag GmbH, D-69451 Weinheim, 1998
0947-6539/98/0407-1262 $ 17.50+.50/0 *Chem. Eur. J.* **1998**, *4*, No. 7

dbc^{2-} are very likely to play any significant role in the intradiol cleavage reaction of **2** with molecular oxygen. The thermodynamic data presented here, however, provide no insight into the question of how easily the monodentate coordination mode of the dioxolene moiety can be achieved in solution, that is whether an open coordination site at the octahedral iron ion is accessible so that a direct attack of an oxygen molecule on the iron site is possible.

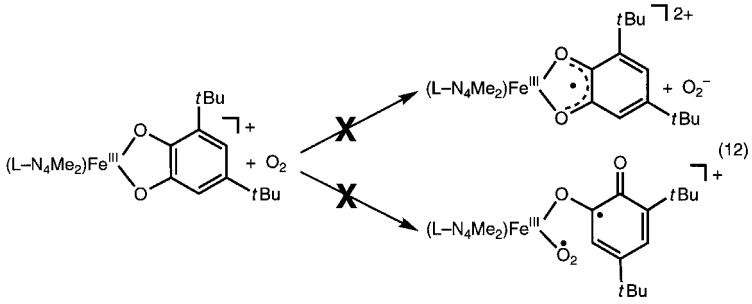

(12)

Reactivity with molecular oxygen and superoxide: Upon exposing a solution of **3a** in acetonitrile to air, the intensity of the absorption band attributed to the iron(III) semiquinonate species decreases to about 90% of its original intensity within the first 24 h and then stays approximately constant. This behavior indicates that the semiquinonate coordinated to an iron(III) ion, by itself, does not react with molecular oxygen, while the reaction of complex **2** with air is essentially complete within 3 h. On the other hand, the iron(II) catecholate complex [Fe(L-N_4Me_2)(dbc)] obtained by the reduction of **2** reacts immediately with air.[8] The electronic absorption spectrum of the solution resulting from the reaction of the iron(II) complex [Fe(L-N_4Me_2)(dbc)] with oxygen reveals the immediate formation of complex **2** in 47% yield. It is noteworthy that, in contrast to a recently reported iron(II) monohydrogencatecholate complex by Que et al.,[20] the iron(III) catecholate complex **2** is *not* formed in 100% yield. These results demonstrate that particular oxidation states of *both* the metal ion *and* the coordinated dioxolene unit are crucial for the occurrence of any cleavage of the *intradiol* C–C bond by molecular oxygen.

In a further experiment, the addition of equivalent amounts of potassium superoxide to a solution of the iron(III) semiquinonate **3** in acetonitrile, through which a stream of nitrogen is vigorously bubbled to expel any generated oxygen in solution, afforded complex **2** in quantitative yields (based on the electronic absorption spectrum). As expected on the basis of the redox potentials ($E_{1/2}(O_2/O_2^-) = -0.87$ V), the equilibrium of the electron transfer in Equation (11) lies on

$$[Fe(L\text{–}N_4Me_2)(dbsq)]^{2+} + O_2^- \longrightarrow [Fe(L\text{–}N_4Me_2)(dbc)]^{+} + O_2 \quad (11)$$

the side of the iron(III) catecholate complex **2** and molecular oxygen. A similar reduction of an iron(III) semiquinonate complex by a superoxide anion has been observed for the complexes [Fe(salen)(dbsq)] (H_2salen = ethylenebis(salicylaldimine))[7c] and [Fe(L)(dbsq)] (H_2L = *N*,*N*′-bis((3-*tert*-butyl-2-hydroxy-5-methylphenyl)methyl)-*N*,*N*′-bismethyl-1,2-diaminoethane)[10d]; however, it should be pointed out that, in contrast to complex **2**, the resulting iron(III) catecholate complexes $[Fe(salen)(dbc)]^-$ and $[Fe(L)(dbc)]^-$ do not react at all with molecular oxygen.[7c]

Thus, this finding provides evidence that the well-established *intradiol* ring cleavage reaction of **2** with molecular oxygen[5] does not occur by an initial electron transfer step [reverse of Equation (11)] to produce iron(III) semiquinonate **3** or a ternary semiquinonato superoxo iron(III) complex as the intermediate [Eq. (12)], but instead by the direct attack of the oxygen molecule onto the iron(III) catecholate moiety. This conclusion is also supported by the finding that the spectrophotometric investigation of the reaction of **2** with molecular oxygen does not provide any indication for an absorption band originating from an intermediary formation of **3**. On the other hand, under an anaerobic atmosphere, complex **3** and the reaction in Equation (1) may be integral parts in a mechanism for the iron-mediated oxidation of catechol derivatives to *o*-benzoquinones by electron-oxidants.

Conclusion

We have synthesized and isolated the first (to the best of our knowledge) low-spin iron(III) semiquinonate complex [Fe(L-N_4Me_2)(dbsq)]$^{2+}$ (**3**) in which the iron ion is bound to the tetraazamacrocycle L-N_4Me_2 and to the bidentate 3,5-di-*tert*-butylsemiquinonate radical in a pseudo-octahedral coordination geometry. The oxidation and spin states of the iron ion and the dioxolene moiety were unambiguously established by structural and Mössbauer spectroscopic evidence. The complex is characterized by a strong antiferromagnetic coupling between the $S = 1/2$ spin of the coordinated semiquinonate radical and the $S = 1/2$ spin state of the low-spin iron(III) ion, which yields a diamagnetic ground state. In acetonitrile, complex **3** reacts within a reversible equilibrium to the low-spin bis(acetonitrile)iron(II) complex **5** and uncoordinated 3,5-di-*tert*-butylbenzoquinone [Eq. (1)]. The thermodynamics and kinetics of this equilibrium reaction were thoroughly investigated by NMR and electrochemical methods. The determination of the equilibrium constant of Equation (1) allows the calculation of the free energies for the complexation reactions of $dbsq^-$ and dbc^{2-} by [Fe(L-N_4Me_2)$(MeCN)_2$]$^{2+,\,3+}$ ions. The reactivity studies of complex **3** with molecular oxygen and with superoxide, respectively, show that complex **3** is not involved in the reaction mechanism of the respective iron(III) catecholate **2** with molecular oxygen, and that the correct oxidation states of *both* the iron ion *and* the dioxolene moiety are required in order for the biomimetic oxygenation reaction of the coordinated catecholate to occur.

Experimental Section

Physical methods: ^{1}H NMR: Bruker AM360; UV/Vis: Varian Cary 5E; IR: Perkin–Elmer 1700X FT-IR and Perkin–Elmer 1720 FT-IR; resonance Raman: Jobin Yvon Ramanon U1000. The spectra were recorded with a rotating device at room temperature on ring-shaped powder pellets

of the sample in a sodium sulfate matrix. The frequencies were calibrated against the 992 cm^{-1} Raman line arising from sodium sulfate. Mössbauer spectra were recorded with a conventional spectrometer in the constant acceleration mode. Isomer shifts are given relative to α-Fe at room temperature. The spectra obtained at low fields (20 mT) were measured in a He bath cryostat (Oxford Instruments, HD 306), equipped with a pair of circular permanent magnets. For high-field spectra a cryostat with a superconducting magnet was used (Oxford Instrument). The spectra were analyzed by least-squares fits and a Lorentzian line shape. Electrochemistry: PAR Model 270 Research Electrochemistry Software controlled Potentiostat/Galvanostat 273A with the electrochemical cell placed in a glovebox. Electrochemical experiments were performed on 1–2 mM acetonitrile solutions containing 0.2 M $(Bu_4N)ClO_4$ as the supporting electrolyte; a higher than normal electrolyte concentration was applied to minimize solution resistance. All potentials were measured vs. a SCE reference electrode at 25 °C. The potentials were not corrected for junction potentials. A Pt-foil electrode was employed as the working electrode. Under these conditions, the potential for the ferrocene/ferrocenium ion couple was 0.43 V. Coulometric experiments were performed with a Pt-gauze electrode. The electrolyses at low temperatures were carried out in a double-jacketed electrolysis cell connected to a Lauda Ultrakryomat RUK 90. Simulated cyclic voltammograms were calculated with the program DigiSim 2.1. Magnetic susceptibilities: SQUID magnetometer (MPMS, Quantum Design) at 2–295 K in an applied field of 1 T. The values for the diamagnetic susceptibilities of the ligand L-N_4Me_2 and of the other components of the complexes were taken from the literature.[21]

Preparation of compounds: The tetraazamacrocyclic ligand L-N_4Me_2 was synthesized according to published procedures, but with some slight modifications.[22] The iron(III) catecholate complexes $[Fe(L\text{-}N_4Me_2)(cat)](BPh_4)$ (**1**·BPh_4) and $[Fe(L\text{-}N_4Me_2)(dbc)](BPh_4)$ (**2**·BPh_4) were prepared as described.[5] All other chemicals were obtained from commercial sources and used without further purification. Acetonitrile was dried over CaH_2 and freshly distilled prior to use in electrochemical experiments.

$[Fe(L\text{-}N_4Me_2)(dbsq)](ClO_4)_2 \cdot 2.5H_2O$ (3a): Under an atmosphere of pure N_2, a solution of L-N_4Me_2 (134 mg, 0.5 mmol) in 96 % ethanol (20 mL) was treated with an ethanolic solution (10 mL) of $[Fe(H_2O)_6](ClO_4)_2$ (181 mg, 0.5 mmol). The mixture was heated to reflux temperatures and then cooled again to room temperature to afford a yellow solution. Dropwise addition of 3,5-di-*tert*-butyl-1,2-benzoquinone (110 mg, 0.5 mmol) in ethanol (15 mL) resulted in the immediate formation of a blue solution, which was heated to reflux temperatures and then slowly cooled to room temperature. The crystalline material obtained by storage of the solution at −30 °C for 1 d was collected under N_2 by filtration and then washed with ether and dried in vacuo to give an analytically pure product. Yield: 331 mg (78 %), dark blue crystals; IR (KBr) (strong bands only): $\tilde{\nu} = 2961, 2871, 1663, 1606, 1583, 1478, 1447, 1424, 1375, 1278, 1242, 1095, 1028, 1000, 980, 876, 800, 760, 637, 626\ cm^{-1}$; $C_{30}H_{45}Cl_2FeN_4O_{12.5}$ (788.46): calcd C 45.70, H 5.75, N 7.11. found: C 45.73, H 5.74, N 7.15.

Warning: Perchlorate salts are potentially explosive and should be handled with care.[23]

$[(L\text{-}N_4Me_2)Fe(dbsq)](PF_6)_2$ (3b): Compound **3b** was prepared by a slightly modified procedure starting with a methanolic solution of iron(II) hexafluorophosphate, which was obtained by treatment of a solution of $FeCl_2 \cdot 4H_2O$ in methanol with silver hexafluorophosphate (2 equiv) under exclusion of light and subsequent filtration of the resulting solution. To this iron(II) hexafluorophosphate solution was added 3,5-di-*tert*-butylbenzoquinone, and the volume of the blue solution was then reduced. Subsequent storage of the solution at −30 °C afforded single crystals suitable for X-ray structural investigations.

Preparation of the ^{57}Fe-enriched samples: $^{57}Fe_2O_3$ was converted to $^{57}FeCl_3 \cdot x H_2O$ by treatment with concentrated HCl and subsequent evaporation to dryness. ^{57}Fe-enriched complex **3** was electrochemically prepared in acetonitrile by oxidation of $[^{57}Fe(L\text{-}N_4Me_2)(dbc)](BPh_4)$ (prepared from $^{57}FeCl_3 \cdot x H_2O$ according to published procedures).[5]

Solutions of $[Fe(L\text{-}N_4Me_2)(sq)]^{2+}$ (4) in acetonitrile: Complex **4** was prepared at −30 °C by electrochemical oxidation of a solution of **1**·BPh_4 at an applied potential of $E = 0.62$ V vs. SCE. Solutions of ^{57}Fe-enriched **4** were analogously prepared from ^{57}Fe-enriched **1**·BPh_4.

Crystal data of 3b: Formula $C_{30}H_{40}F_{12}FeN_4O_2P_2$; $M_r = 834.45$; crystal dimensions: $0.1 \times 0.1 \times 0.6$ mm; crystal system monoclinic; space group $P2_1/c$ (No. 14); cell dimensions: $a = 14.868(4)$, $b = 10.117(2)$, $c = 23.673(3)$ Å, $\beta = 98.08(1)°$; $V = 3526(1)$ Å^3; $\rho_{calcd} = 1.572\ g\,cm^{-3}$; $Z = 4$; $F(000) = 1712$, graphite-monochromated $Cu_{K\alpha}$ radiation ($\lambda = 1.54178$ Å); $\mu = 51.92\ cm^{-1}$; $T = 153$ K; Enraf–Nonius CAD 4 diffractometer; $\omega - 2\theta$ scans in the range $6 \le 2\theta \le 120°$; 5235 unique reflections (3454 reflections with $F_o > 4\sigma(F_o)$); 594 variables (336 restraints); GooF on F^2 ($F_o > 4\sigma(F_o)$) = 1.150; extinction coefficient = 0.00004(2); R ($F_o > 4\sigma(F_o)$) = 4.98 % with $R = \Sigma\,||F_o| - |F_c||/\Sigma\,|F_o|$; wR^2 ($F_o > 4\sigma(F_o)$) = 10.27 % with $wR^2 = \{\Sigma[w(F_o^2 - F_c^2)^2]/\Sigma[w(F_o^2)^2]\}^{1/2}$; largest peak (hole) = 0.32 (−0.33) e Å^{-3}. Empirical absorption correction on the data set was performed with the program XEMP. The positions of the non-hydrogen atoms were determined by SHELXS 86[24] and by Fourier difference maps by the program SHELXL-93.[24] The structural parameters were refined with the program SHELXL-93, which used F^2 of all symmetry-independent reflections except those with very negative F^2 values. All non-hydrogen atoms were refined anisotropically. The two hexafluorophosphate anions are severely disordered and were modeled by two separate molecules for each site. The P–F and F–F distances were restrained to yield ideal octahedral geometries for these anions. Hydrogen atoms were assigned idealized locations and their isotropic temperature factors were refined.

Crystallographic data (excluding structure factors) for the structure reported in this paper have been deposited with the Cambridge Crystallographic Data Centre as supplementary publication no. CCDC-100827. Copies of the data can be obtained free of charge on application to CCDC, 12 Union Road, Cambridge CB2 1EZ, UK (fax: (+ 44) 1223-336-033; e-mail: deposit@ccdc.cam.ac.uk).

Acknowledgements: This work was supported by a grant from the Deutsche Forschungsgemeinschaft. Furthermore, we are very grateful to Dr. M. Rudolph from the Friedrich-Schiller-Universität in Jena for lending us his program DigiSim 2.1.

Received: October 29, 1997 [F870]

[1] a) G. Avigad, D. Amaral, C. Asensio, B. Horecker, *J. Biol. Chem.* **1962**, *237*, 2736; b) M. M. Whittaker, J. W. Whittaker, *ibid.* **1988**, *263*, 6074; c) M. M. Whittaker, J. W. Whittaker, *ibid.* **1990**, *265*, 9610; d) M. M. Whittaker, Y.-Y. Chuang, J. W. Whittaker, *J. Am. Chem. Soc.* **1993**, *115*, 10029; e) G. T. Babcock, M. K. El-Deeb, P. O. Sandusky, M. M. Whittaker, J. W. Whittaker, *ibid.* **1992**, *114*, 3727.

[2] a) J. A. Halfen, V. G. Young, W. B. Tolman, *Angew. Chem* **1996**, *108*, 1832; *Angew. Chem. Int. Ed. Engl.* **1996**, *35*, 1687; b) Y. Wang, T. D. P. Stack, *J. Am. Chem. Soc.* **1996**, *118*, 13097; c) B. Adams, E. Bill, E. Bothe, B. Goerdt, G. Haselhorst, K. Hildenbrand, A. Sokolowski, S. Steenken, T. Weyhermüller, K. Wieghardt, *Chem. Eur. J.* **1997**, *3*, 308; d) A. Sokolowski, H. Leutbecher, T. Weyhermüller, R. Schnepf, E. Bothe, E. Bill, P. Hildebrandt, K. Wieghardt, *JBIC* **1997**, *2*, 444; e) J. A. Halfen, B. A. Jazdzewski, S. Mahapatra, L. M. Berreau, E. C. Wilkinson, L. Que, Jr., W. B. Tolman, *J. Am. Chem. Soc.* **1997**, *119*, 8217.

[3] M. Sono, M. P. Roach, E. D. Coulter, J. H. Dawson, *Chem. Rev.* **1996**, *96*, 2841.

[4] a) L. Que, Jr. in *Iron Carriers and Iron Proteins* (Ed.: T. M. Loehr), VCH, New York, **1989**, p. 467; b) D. D. Cox, L. Que, Jr., *J. Am. Chem.Soc.* **1988**, *110*, 8085; c) H. G. Jang, D. D. Cox, L. Que, Jr., *ibid.* **1991**, *113*, 9200.

[5] W. O. Koch, H.-J. Krüger, *Angew. Chem.* **1995**, *107*, 2928; *Angew. Chem. Int. Ed. Engl.* **1995**, *34*, 2671.

[6] For comprehensive reviews on metal complexes with dioxolene ligands see: a) C. G. Pierpont, C. W. Lange, *Prog. Inorg. Chem.* **1994**, *41*, 331; b) C. G. Pierpont, R. M. Buchanan, *Coord. Chem. Rev.* **1981**, *38*, 45.

[7] a) S. R. Boone, G. H. Purser, H.-R. Chang, M. D. Lowery, D. N. Hendrickson, C. G. Pierpont, *J. Am. Chem. Soc.* **1989**, *111*, 2292; b) R. B. Lauffer, R. H. Heistand, II, L. Que, Jr., *Inorg. Chem.* **1983**, *22*, 50; c) R. B. Lauffer, R. H. Heistand, II, L. Que, Jr., *J. Am. Chem. Soc.* **1981**, *103*, 3947.

[8] W. O. Koch, H.-J. Krüger, unpublished results.

[9] W. O. Koch, V. Schünemann, M. Gerdan, A. X. Trautwein, H.-J. Krüger, *Chem. Eur. J.* **1998**, *4*, 686.

 © WILEY-VCH Verlag GmbH, D-69451 Weinheim, 1998 0947-6539/98/0407-1264 $ 17.50+.50/0

[10] a) A. S. Attia, S. Bhattacharya, C. G. Pierpont, *Inorg. Chem.* **1995**, *34*, 4427; b) A. S. Attia, O. S. Jung, C. G. Pierpont, *Inorg. Chim. Acta* **1994**, *226*, 91; c) R. M. Buchanan, S. L. Kessel, H. H. Downs, C. G. Pierpont, D. N. Hendrickson, *J. Am. Chem. Soc.* **1978**, *100*, 7894; d) P. Mialane, E. Anxolabéhère-Mallart, G. Blondin, A. Nivorojkine, J. Guilhem, L. Tchertanova, M. Cesario, N. Ravi, E. Bominaar, J.-J. Girerd, E. Münck, *Inorg. Chim. Acta* **1997**, *263*, 367.

[11] a) H.-J. Krüger, *Chem. Ber.* **1995**, *128*, 531; b) H. Kelm, H.-J. Krüger, *Inorg. Chem.* **1996**, *35*, 3533.

[12] a) D. D. Cox, S. J. Benkovic, L. M. Bloom, F. C. Bradley, M. J. Nelson, L. Que, Jr., D. E. Wallick, *J. Am. Chem. Soc.* **1988**, *110*, 2026; b) K. Nakamoto, *Infrared Spectra of Inorganic and Coordination Compounds*, Wiley-Interscience, **1986**, p. 245; c) D. M. Adams, *Metal–Ligand and Related Vibrations*; Arnold; London, **1967**; d) S. Salama, J. D. Stong, J. B. Neilands, T. G. Spiro, *Biochemistry* **1978**, *17*, 3781.

[13] a) Y. Tomimatsu, S. Kint, J. R. Scherer, *Biochemistry* **1976**, *15*, 4918; b) L. Que, Jr., *Struct. Bonding* **1980**, *40*, 39.

[14] A. Dei, D. Gatteschi, L. Pardi, *Inorg. Chem.* **1993**, *32*, 1389.

[15] a) C. Benelli, A. Dei, D. Gatteschi, L. Pardi, *Inorg. Chem.* **1989**, *28*, 1476; b) C. Benelli, A. Dei, D. Gatteschi, H. Gudel, L. Pardi, *ibid.* **1989**, *28*, 3089; c) C. Benelli, A. Dei, D. Gatteschi, L. Pardi, *Inorg. Chim. Acta* **1989**, *163*, 99; d) C. Benelli, A. Dei, D. Gatteschi, L. Pardi, *Inorg. Chem.* **1988**, *27*, 2831.

[16] a) M. E. Bodini, G. Copia, R. Robinson, D. T. Sawyer, *Inorg. Chem.* **1983**, *22*, 126; b) M. D. Stallings, M. M. Morrison, D. T. Sawyer, *ibid.* **1981**, *20*, 2655.

[17] a) M. Haga, E. S. Dodsworth, A. B. P. Lever, *Inorg. Chem.* **1986**, *25*, 447; b) H. Masue, A. B. P. Lever, P. R. Auburn, *ibid.* **1991**, *30*, 2402; b) D. J. Stufkens, T. L. Snoeck, A. B. P. Lever, *ibid.* **1988**, *27*, 953.

[18] M. Haga, K. Isobe, S. R. Boone, C. G. Pierpont, *Inorg. Chem.* **1990**, *29*, 3795.

[19] F. Hartl, A. Vlcek, Jr., *Inorg. Chem.* **1992**, *31*, 2869.

[20] Y.-M. Chiou, L. Que, Jr., *Inorg. Chem.* **1995**, *34*, 3577.

[21] a) *Landolt–Börnstein Vol. II/10* (6th edition) (Eds.: K.-H. Hellwege, A. M. Hellwege), Springer, Berlin, **1967**; b) *Landolt–Börnstein New Series Vol. II/8* Supplement 1 (Eds.:K.-H. Hellwege, A. M. Hellwege), Springer, Berlin, **1976**; c) H.-J. Krüger, *Chem. Ber.* **1995**, *128*, 531.

[22] a) B. Alpha, E. Anklam, R. Deschenaux, J.-M. Lehn, M. Pietraskiewicz, *Helv. Chim. Acta* **1988**, *71*, 1042; b) F. Bottino, M. Di Grazia, P. Finocchiaro, F. R. Fronczek, A. Mamo, S. Pappalardo, *J. Org. Chem.* **1988**, *53*, 3521.

[23] a) W. C. Wolsey, *J. Chem. Educ.* **1973**, *50*, A335; b) K. N. Raymond, *Chem. Eng. News* **1983**, *61*, (Dec. 5), 4.

[24] SHELXS-86: Crystal Structure Solution Program, G. M. Sheldrick, Göttingen (Germany), **1986**; G. M. Sheldrick, in *Crystallographic Computing 3*; (Eds.: G. M. Sheldrick, C. Krüger, R. Goddard), Oxford University Press, **1985**, pp. 175; SHELXL-93: Crystal Structure Refinement Program, G. M. Sheldrick, Göttingen (Germany), **1993**.